

# A SOLID STATE OPENING SWITCH FOR CROWBAR REPLACEMENT

Ian S. Roth, Marcel P.J. Gaudreau, Michael A. Kempkes  
Diversified Technologies, Inc. Bedford, MA USA

## Abstract

Opening switches have substantial advantages over crowbars. Diversified Technologies has developed solid-state opening-switches using series arrays of IGBTs; many systems have been delivered. The control circuitry has been improved, and the current capability of low-cost switches has been increased from 5 to 25 A. The opening switch being developed will be part of a complete klystron power-supply system for the Advanced Photon Source at Argonne National Laboratory.

## INTRODUCTION

Crowbars are commonly used to protect klystrons from arc damage. When an arc occurs, the crowbar closes, and rapidly discharges the energy-storage capacitor. A typical crowbar circuit diagram is shown in Figure 1. An alternative way to protect a klystron is to use a switch that opens during an arc (also shown in Figure 1). Opening switches have substantial advantages over crowbars:

- No series resistor is required, so an opening-switch system has higher circuit efficiency.
- Because the energy-storage capacitor does not discharge during an arc, high voltage (and RF) can be turned back on in less than 30  $\mu\text{s}$ , before the circulating accelerator beam dumps [1]; see Figure 2. No beam restart is required.
- Crowbars use mercury-containing ignitrons. When an ignitron fails, the required clean-up can be time-consuming and costly. As an example, the ignitron failure at the Joint European Tokamak in 1986 shut down the machine for three months. The total cost of the failure, including lost staff time, was £1 M (\$1.9 M) [2]. Opening switches use no mercury.

Opening switches can be made using vacuum tubes, but these are expensive, have a large forward voltage drop (10-20% of the total switched voltage), and a limited lifetime. Diversified Technologies has developed opening switches made from a series array of solid-state devices, IGBTs or FETs. These are much less expensive than vacuum tubes, and have much

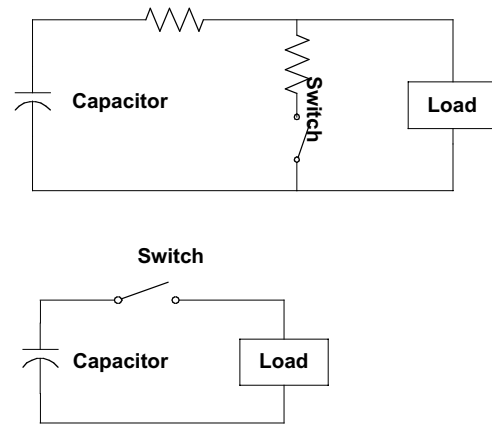


Fig. 1. Circuit diagrams for crowbar (upper) and opening switch (lower).

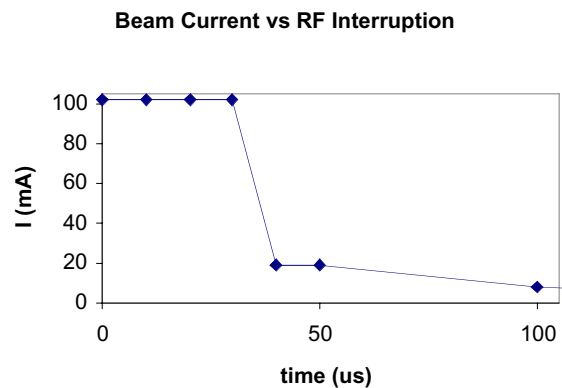


Fig. 2. Beam current vs. RF interruption. An interruption of up to 30  $\mu\text{s}$  can be sustained without beam loss.

longer lifetimes. The forward voltage drop of these opening switches is small, less than 0.5% of the opening switch voltage. Opening switches have been in service for several years without any failures from non-simultaneous opening. An additional benefit of the series-array opening switch is redundancy. Switches are made with excess voltage capability, so the switch can continue operating even if several devices should fail. Diagnostics report any device failures, so repairs can be scheduled appropriately.

### OPENING SWITCH OPERATION

An example of an operational opening switch is shown Figure 3 (left). This switch is also used as a modulator, like most of the high-power opening switches delivered. It carries 500 A and opens to

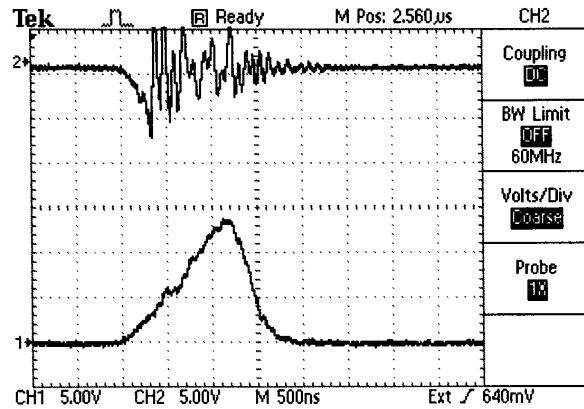


Fig. 3. Left: Opening switch delivered to CPI. Right: Waveforms of a deliberate short. Upper trace, voltage, 50kV/division; lower trace, current, 250 A/division.

140 kV. The unit has been operating at CPI for several years. Waveforms of a deliberate short are shown in Figure 3 (right). The lower trace shows the current. After the current passes the arc-detection threshold of 200 A, it rises for an additional 700 ns before being interrupted. The peak current interrupted is 700 A.

### OPENING SWITCH DEVELOPMENT

We are developing opening switches further under a Phase-II SBIR grant from the DOE. There are two directions for the development: improving the control circuitry, and reducing the cost of the specific opening switch.

One of the ways we have developed the control circuitry is to use DC current monitors that have a fast response. In a DC system (often used to drive klystrons) pulsed current transformers do not work well. This is because the ferrite in the transformer saturates, and the transformer will not respond to pulsed fault currents. The pulse response of the LEM DC current monitor (see Figure 4) is fast enough for fault detection.

We have further developed the control circuitry to decrease the system response time to an over-current fault.

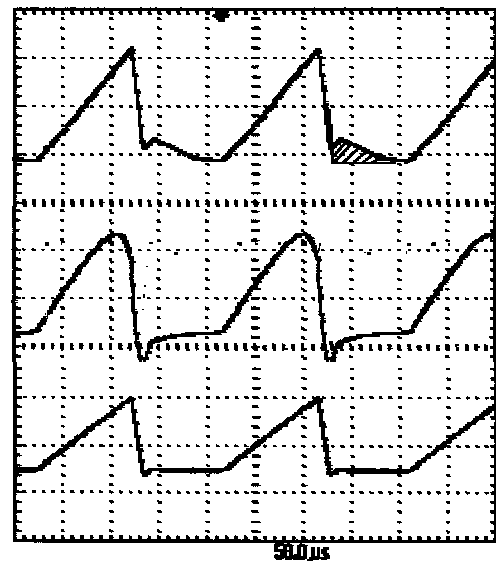


Fig. 4. Identical current waveform with three different diagnostics. Peak current is 30 A; timescale is 50  $\mu$ s/division. Upper trace, LEM-100P; middle trace: Pearson 110 transformer; lower trace, Pearson 1025 current transformer.

This has been done by using faster fiber-optic receivers (fiber optic cables are used to trigger and diagnose the IGBTs) and increasing the slewing rate of the IGBT trigger. DTI systems presently take 700 ns from the over-current signal to the turn-off of the switch.

We have also added fault latching, which displays the first fault signal, and locks out subsequent signals. This allows the operator to determine the cause of a fault, and make repairs if needed. Finally, we have reduced the number of fiber-optic cables per switch plate from three to two by multiplexing diagnostic signals.

As well as improving the control circuitry, we are increasing the DC capability of low-cost opening switches (Figure 5) from 5 to 25 A. These switches use discrete IGBTs, and are substantially less expensive than ones using IGBT modules. The low-cost opening switch will be incorporated into the klystron power-supply for the Advanced Photon Source (APS) at Argonne National Lab.



Figure 5. Low-cost switch module.

To increase the current capability of the low-cost opening switches, we first selected the best IGBT available. The properties of various devices are compared in Table 1.

Table 1 Comparison of discrete IGBTs.  $R_{JC}$  is the thermal resistance from junction to case;  $R_{CK}$  is the thermal resistance from case to heat sink.

Device	$V_{max}$ (V)	$I_{max DC}$ (A)	$V_{forward}$ (V)	$R_{JC}$ ( $^{\circ}C/W$ )	$R_{CK}$ ( $^{\circ}C/W$ )	$t_{current\ delay\ off} + t_{current\ fall}$ (ns)
Fairchild HGTG 30N120CN	1200	75	2.1	0.25	0.25	400
IXYS IXLF 19N250A	2500	32	3.2	0.5	0.25	650
IXYS IXGH 45N120	1200	75	2.5	0.42	0.25	760
IR IRG4PH50S	1200	57	1.75	0.64	0.25	2170
IR IRG4PH50U	1200	45	3.20	0.64	0.25	600
APT 50GF120LR	1200	80	2.9	0.32	0.25	430

We chose the Fairchild (formerly Intersil) 30N120CN; it has the lowest thermal resistance and the second-lowest forward voltage drop of the devices available. While the IXYS 19N250A operates at 2500 V instead of 1200 V, the forward voltage drop and thermal resistance of this device are too large to permit operation at the required 20 A DC.

Having selected the IGBT, we investigated heat sinks. The heat sink performance was measured by mounting the sink to an IGBT, lowering the assembly in oil, passing current through the IGBT, and measuring the temperature rise. A selection of the heat sinks we considered is listed in Table 2.

Table 2. Heat sink performance.

No.	Mat'l	Base area (in <sup>2</sup> )	Height, fin gap, fin thickness (in)	$R_{s, still\ oil}$ , $^{\circ}C/W$	$R_{s, moderately\ flowing\ oil}$ , $^{\circ}C/W$	$R_{s, rapidly\ flowing\ oil}$ , $^{\circ}C/W$
1	Al	0.79	2 0.094 0.063	1.40	0.86	-
3	Al	6.8	1.3 0.25 0.063	0.36	0.21	0.13
5	Cu	6	2.2 0.125 0.063	0.24	0.12	-
9	Al	6.2	1.6 0.19 0.11	-	0.13	-

Heat sink 1, which we have been using, has the highest thermal resistance of the sinks tested. Heat sink 3 was made from extruded aluminum. Note that the thermal resistance was lower when the oil was flowing rapidly (with the device directly at the exhaust of the oil pump) than when the oil was flowing moderately (with the device 18" away from the pump exhaust). We decided, however, that rapidly-flowing oil would be impractical. Heat sink 5 was made from copper. While this heat sink has a low thermal resistance, it was expensive to manufacture, and we decided to use extruded-aluminum heat sinks. Heat sink 9 has a low thermal resistance,  $0.13^{\circ}\text{C/W}$ . Using heat sink 9A, which is made from the same extrusion as heat sink 9 but with half the base area, halves the size of the opening switch while giving only a  $7^{\circ}\text{C}$  increase in temperature. The calculated IGBT-junction temperature rise is then  $2.7\text{ V} \times 20\text{ A} \times (0.50 + 0.26)\text{ }^{\circ}\text{C/W} = 41^{\circ}\text{C}$ .

### ARGONNE KLYSTRON POWER-SUPPLY SYSTEM

The opening switch is the first part of a klystron power-supply system we are building for APS. Specifications for the system are listed in Table 3.

Table 3. Specifications for the APS Klystron Power Supply at Argonne.

Component	Specification
Transformer	13.6 kV in, 110 kV out, 2.2 MW
Buck regulator	110 kV in, 0-100 kV out, 20 A out, $\pm 0.5\%$ regulation, $>90\%$ efficient
Filament heater	0-25 V, 0-25 A, $\pm 1\%$ current regulation
Mod anode power supply	0-90 kV with respect to cathode, 20 mA
Opening switch	100 kV, 20 A, 1 $\mu\text{s}$ response to fault
Ion pump power supply	3.5 - 5.5 kV, 20 mA
Electromagnet power supplies	0-300 V, 0-12 A, 0.1% current regulation
Controls	interlocks, local/remote operation

In addition to the opening switch, the other potentially difficult component could be the buck regulator. The same technology used for the switch, however, is used for the buck regulator, and the required performance has already been demonstrated: Figure 6 shows a buck regulator that is installed at CPI. This buck regulator gives a power output of 140 kV and 20 A, with regulation to  $\pm 0.3\%$ .

The remaining components in the system use conventional technology. We anticipate no difficulty in constructing the complete APS klystron power-supply.

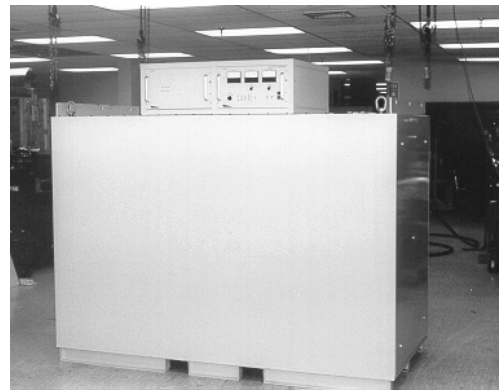


Figure 6. Buck regulator installed at CPI.

### REFERENCES

- [1] Doug Horan, Advanced Photon Source, Argonne National Laboratory; private communication.
- [2] Geoff Pile, Advanced Photon Source, Argonne National Laboratory; private communication.